

# New brown dwarf disks in Upper Scorpius observed with WISE

P. Dawson,<sup>1\*</sup> A. Scholz,<sup>1</sup> T.P. Ray,<sup>1</sup> K.A. Marsh,<sup>2</sup> K. Wood,<sup>3</sup> A. Natta,<sup>1,4</sup>  
D. Padgett,<sup>5</sup> M.E. Ressler.<sup>6\*</sup>

<sup>1</sup>*School of Cosmic Physics, Dublin Institute for Advanced Studies, 31 Fitzwilliam Place, Dublin 2, Ireland*

<sup>2</sup>*School of Physics and Astronomy, Cardiff University, Cardiff CF24 3AA, UK*

<sup>3</sup>*School of Physics and Astronomy, University of St. Andrews, North Haugh, St. Andrews KY16 9SS, UK*

<sup>4</sup>*INAF - Osservatorio Astrofisico di Arcetri, Largo E. Fermi 5, 50125 Firenze, Italy*

<sup>5</sup>*Goddard Space Flight Center, Greenbelt, MD 20771, USA*

<sup>6</sup>*Jet Propulsion Laboratory, California Institute of Technology, 4800 Oak Grove Drive, Pasadena, CA 91109, USA*

Accepted 2012 xxxxxxxx xx. Received 2012 xxxxxxxx xx; in original form 2012 October xx

## ABSTRACT

We present a census of the disk population for UKIDSS selected brown dwarfs in the 5–10 Myr old Upper Scorpius OB association. For 116 objects originally identified in UKIDSS, the majority of them not studied in previous publications, we obtain photometry from the WISE database. The resulting colour-magnitude and colour-colour plots clearly show two separate populations of objects, interpreted as brown dwarfs with disks (class II) and without disks (class III). We identify 27 class II brown dwarfs, 14 of them not previously known. This disk fraction (27 out of 116 or 23%) among brown dwarfs was found to be similar to results for K/M stars in Upper Scorpius, suggesting that the lifetimes of disks are independent of the mass of the central object for low-mass stars and brown dwarfs. 5 out of 27 disks (19%) lack excess at 3.4 and 4.6  $\mu\text{m}$  and are potential transition disks (i.e. are in transition from class II to class III). The transition disk fraction is comparable to low-mass stars. We estimate that the timescale for a typical transition from class II to class III is less than 0.4 Myr for brown dwarfs. These results suggest that the evolution of brown dwarf disks mirrors the behaviour of disks around low-mass stars, with disk lifetimes on the order of 5–10 Myr and a disk clearing timescale significantly shorter than 1 Myr.

**Key words:** techniques: photometric – techniques: brown dwarfs – open clusters and associations: individual: Upper Scorpius – infrared: stars.

## 1 INTRODUCTION

Brown dwarfs – substellar objects with masses below the Hydrogen burning limit of  $0.08 M_{\odot}$  – are ideal to test the mass dependence of critical parameters in stellar evolution. One example for such a parameter is the lifetime of circumstellar disks, which is an important constraint for the core-accretion scenarios for planet formation. The disk lifetime is affected by a number of physical processes, e.g. disk ionisation by the central object and cosmic rays, accretion, grain growth (e.g. Dullemond et al. (2007)). Our understanding of the relative importance of these processes and how they change with

object mass is still incomplete, i.e. observational guidance is important to advance the theory.

The clear majority of low-mass stars lose their disk within less than 5 Myr (Haisch et al. 2001; Jayawardhana et al. 2006). Maybe the best test for the longevity of disks is the Upper Scorpius OB association (UpSco in the following), the oldest nearby star forming region with a substantial number of brown dwarfs. UpSco is often assumed to have an age of 5 Myr (Preibisch et al. 2002) but recently Pecaute et al (2012) have derived an older age of 10 Myr for this region. In UpSco, Carpenter et al. (2006) derived a disk frequency of  $< 8\%$  for F and G stars and  $19 \pm 4\%$  for K0–M5 stars (with  $1\sigma$  binomial confidence intervals). The brown dwarfs in this region exhibit a disk fraction of  $37 \pm 9\%$ , based on an examination of 35 objects (Scholz et al. 2007). Thus, the Spitzer data tentatively shows that the disk fractions *in UpSco increase*

\* E-mail: pdawson@cp.dias.ie (PD); aleks@cp.dias.ie (AS); tr@cp.dias.ie (TR); ken.marsh@astro.cf.ac.uk (KM); kw25@st-andrews.ac.uk (KW); natta@arcetri.astro.it (AN); dlp@ipac.caltech.edu (DP); michael.e.ressler@jpl.nasa.gov (MR)

monotonically with decreasing object mass for early *F*- to late *M*-type objects. This would imply a mass dependence in the disk evolution, resulting in long-lived disks in the substellar regime.

So far, the brown dwarf disk frequency in UpSco is affected by low number statistics. Here we set out to test previous findings based on a much enlarged number of brown dwarfs in UpSco, identified from UKIDSS. To identify the objects in our sample that have a disk (class II objects) and those that do not (class III objects), we use data from the Wide-Field Infrared Survey Explorer (WISE) (Wright et al. 2010). As will be shown, with improved statistics we find a disk fraction for brown dwarfs that is consistent with the value published for low-mass stars in this region.

## 2 TARGETS

Dawson, Scholz & Ray (2011) identified 19 new brown dwarf candidates in the south of UpSco via a photometric and proper motion analysis of UKIDSS data. The level of contamination from background stars in the sample was shown to be negligible. Using the same method in the north of UpSco a further 49 objects previously identified by Lodieu et al. (2006, 2007) as brown dwarf candidates were recovered. Spectra have been taken of 26 of these 49 objects (Martin et al. 2004; Slesnick et al. 2006; Lodieu et al. 2006, 2008, 2011) and all 26 have been confirmed as brown dwarfs. This provides a sample of 68 very low mass stellar and substellar objects in UpSco. Dawson, Scholz & Ray (2011) determined that the 68 objects ranged in mass from  $0.01 M_{\odot}$  to  $0.09 M_{\odot}$  by comparing their observed *Z* magnitudes with theoretical *Z* magnitudes from the DUSTY models for 5 Myr old objects.

Dawson, Scholz & Ray (2011) used the 8th Data Release from UKIDSS to identify the new brown dwarfs. Since then, UKIDSS has issued a 9th Data Release which covers a substantially larger area in UpSco. Using the same method as in Dawson, Scholz & Ray (2011) we have identified a further 51 objects in the same mass range to add to the sample. The details of this extended survey are given in Appendix A. The addition of these new objects increases the size of the homogeneous sample of objects uniformly selected via their colour and proper motion characteristics to 119. Although some objects in our sample may be slightly above the substellar threshold, we will refer to our targets as “brown dwarfs” throughout this paper, for simplicity.

All 119 objects lie close to the 5 Myr DUSTY model isochrones of Chabrier et al. (2000) in a (*Z*-*J*,*Z*) UKIDSS passbands colour-magnitude diagram, as shown in figure 1, i.e. none of them exhibit any substantial excess at these near infrared wavelengths. The objects are also generally free from reddening caused by extinction (Dawson, Scholz & Ray (2011), also see Appendix A this paper). Consequently it can be inferred that the (*Z*-*J*,*Z*) value for any of the objects is photospheric in origin with negligible contribution from any circum-substellar disk. Thus, the method of selecting these 119 objects is unbiased with respect to the presence of circum-substellar disks.

As pointed out above, the 26 objects in our sample with published spectra have been confirmed to be very low mass members of UpSco. In addition, we have recently obtained

spectra for 25 further objects from this sample; and all of them are confirmed as very low mass members of UpSco as well (Dawson et al., in preparation). Although the spectroscopic follow-up is not yet complete for our sample, the 100% success rate for almost half the sample indicates that our selection method based on photometry and proper motion generates a clean, unbiased sample with negligible contamination by background objects ( $\leq 2\%$ ).

## 3 WISE DATA

For 116 of the 119 targets discussed above we obtained WISE data. The remaining 3 were not listed in the WISE database. For the 116 the 2MASS identifier listed in the WISE database agrees with the one from UKIDSS. In addition, all objects were visually examined in the WISE images and in the UKIDSS images. It was found that for the 116 objects analysed here the identification of the UKIDSS source with the WISE source at the same position is unambiguous (for the three excluded targets this is not the case). Furthermore, since our target fields are sparsely populated and well above the Galactic plane (latitude 10-30 deg), the likelihood of accidental contamination by other objects is very low.

WISE surveyed the whole sky in four mid-infrared wavebands simultaneously, using passbands with effective wavelengths of  $3.4 \mu\text{m}$  (W1),  $4.6 \mu\text{m}$  (W2),  $12 \mu\text{m}$  (W3) and  $22 \mu\text{m}$  (W4). We used the results of profile-fitting photometry from the All Sky Data Release, further details of which can be found in Cutri et al. (2011)<sup>1</sup>. Among the 116 objects are 2 that were previously examined by Scholz et al. (2007) and confirmed to have disks.

## 4 COLOUR ANALYSIS

The five UKIRT passbands; *Z*, *Y*, *J*, *H* and *K* have respective wavelengths of  $0.88 \mu\text{m}$ ,  $1.03 \mu\text{m}$ ,  $1.25 \mu\text{m}$ ,  $1.63 \mu\text{m}$ , and  $2.20 \mu\text{m}$ . Similar *J*, *H* and *K* passbands are also used in 2MASS. As noted above, the four WISE passbands; W1, W2, W3, W4, have longer wavelengths of  $3.4 \mu\text{m}$ ,  $4.6 \mu\text{m}$ ,  $12 \mu\text{m}$  and  $22 \mu\text{m}$  respectively. Different colour-colour and colour-magnitude diagrams using combinations of all nine passbands were examined. The (*Z*-*J*,*Z*) and (W1-W2,*Z*) colour-magnitude diagrams are shown in figure 1. Theoretical isochrones for 5 Myr old sub-stellar objects are also shown over-plotted on the diagrams. These isochrones are based on the DUSTY models derived by Chabrier et al. (2000) and obtained from both I. Baraffe and F. Allard (private communications). The isochrones were computed using both the UKIDSS and WISE filter profiles. The (*Z*-*J*,*Z*) isochrone was used to assign masses to objects by Dawson, Scholz & Ray (2011). The uppermost point on the 5 Myr isochrone corresponds to a mass of  $0.09 M_{\odot}$  while the lowest point corresponds to a mass of  $0.01 M_{\odot}$ .

<sup>1</sup> For more details of the WISE All Sky Data Release also see <http://wise2.ipac.caltech.edu/docs/release/allsky/expsup/>

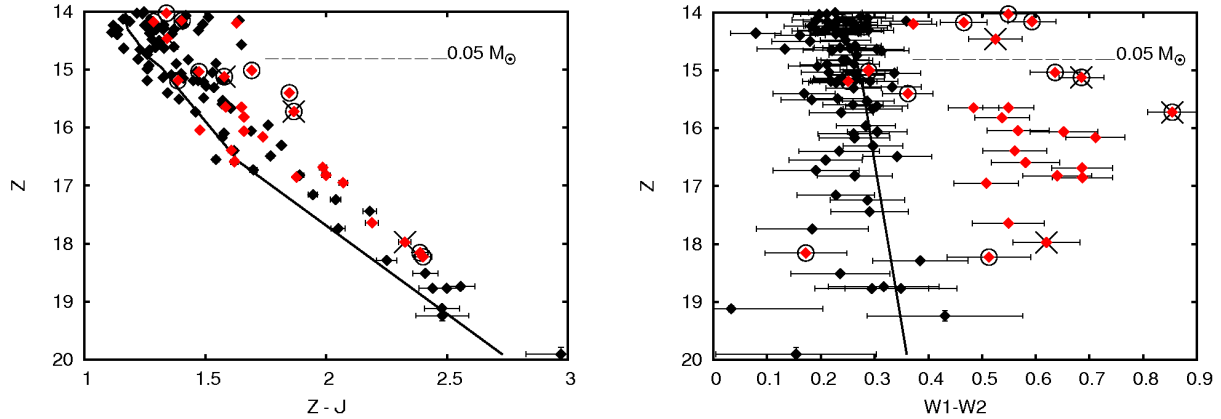


**Figure 1.**  $(Z-J,Z)$  and  $(W1-W2,Z)$  colour-magnitude diagrams for 116 out of 119 brown dwarfs identified in UpSco for which WISE data were available. The class II objects are marked in red in the online version of this paper. The 5 Myr DUSTY model (Chabrier et al. 2000) isochrones are also shown with mass decreasing from  $0.09 M_{\odot}$  (top) to  $0.01 M_{\odot}$  (bottom). The  $0.05 M_{\odot}$  positions on the isochrones are indicated. In the  $(Z-J,Z)$  diagram all the objects are grouped close to the isochrone and none show any significant colour excess. However, two distinct populations of objects are clearly visible in the  $(W1-W2,Z)$  diagram, one close to the isochrone and one showing an excess in  $W1-W2$ . The 11 objects ringed have bright unambiguous signals in  $W4$  ( $22 \mu\text{m}$ ), diagnostic of the presence of a disk (see text; section 4.1.4). The 4 objects marked with a cross have significant variations in their UKIRT and 2MASS J or H magnitudes, a characteristic associated with accretion events or variable extinction (also see text; section 4.2).

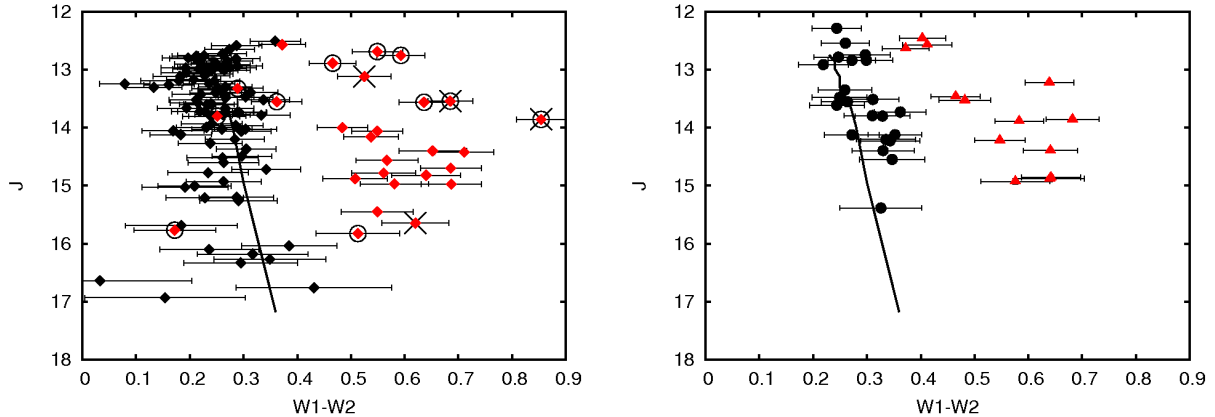


**Figure 2.**  $(W1-W2,J)$  colour-magnitude diagrams. The 116 brown dwarfs with available WISE data analysed in this work are shown in the left panel with symbols and isochrone as in figure 1. The right panel shows the same diagram for 35 objects in UpSco identified in Scholz et al. (2007). Objects confirmed as having disks in Scholz et al. (2007) are shown as closed triangles while those with no disk detected are shown as closed circles. As can be seen, the objects in the population with obvious colour excess all have disks. A few objects with disks exhibit a smaller, but still significant colour excess (i.e. they are more than  $2\sigma$  away from the isochrone). Objects with no disk lie close to the isochrone.

## 4.1 WISE data for UpSco brown dwarfs

### 4.1.1 $W1-W2$ ( $3.4 \mu\text{m}-4.6 \mu\text{m}$ )

In the  $(Z-J,Z)$  diagram all the objects are grouped close to the isochrone and none show any significant colour excess, as discussed above. However, two distinct populations of objects are clearly visible in the  $(W1-W2,Z)$  diagram, one close to the isochrone and one showing an excess in  $W1-W2$  ( $3.4 \mu\text{m}-4.6 \mu\text{m}$ ). The population with excess is best understood as objects harbouring dusty disks and therefore emitting thermal infrared radiation (class II). These two populations do not show up in the diagrams that utilise only UKIRT passbands. Other diagrams that combine both UKIRT and WISE passbands do show the two populations.

Colours that use a UKIRT and WISE  $W1$  ( $3.4 \mu\text{m}$ ) passband do show the two populations but not as clearly as colours incorporating  $W2$  ( $4.6 \mu\text{m}$ ). The  $K-W2$  colour in particular discriminates between the two populations almost as well as the  $W1-W2$  colour. The  $W1-W2$  colour was chosen as the primary diagnostic for distinguishing between class II and class III objects in this work (see figures 1 and 2).

### 4.1.2 $W1-W2$ : Comparison with Scholz (2007)

To test that the method outlined above was successfully discriminating between class II and class III objects it was also applied to the 35 objects in UpSco examined by Scholz et al. (2007). That study used a Spitzer survey combining spec-

**Table 1.** Objects with photometric variability  $>0.2\text{mag}$  in J,H or K.

Name	$\Delta J$	$\Delta H$	$\Delta K$
2MASSJ15514709-2113234	0.84	0.59	0.25
2MASSJ15521088-2125372	0.24	0.11	0.03
2MASSJ15472282-2139141	0.38	0.25	0.21
2MASSJ16030235-2626163	0.17	0.30	0.11

trosopy from 8 to  $12\ \mu\text{m}$  and photometry at  $24\ \mu\text{m}$ . As 33 of the 35 objects lie outside the area covered by UKIDSS there is no Z or Y passband data available for them. However they are recorded in the J, H and K passbands of 2MASS. The 35 objects were plotted in a (W1-W2,J) colour-magnitude diagram (shown in the right panel of figure 2) using data from 2MASS. The 116 objects from this work were also plotted in a (W1-W2,J) colour-magnitude diagram (shown in the left panel of figure 2) for comparison, using data from the UKIDSS J passband. Two of the objects from Scholz et al. (2007) lie inside the area covered by UKIDSS and were re-covered by Dawson, Scholz & Ray (2011). The differences in their UKIDSS and 2MASS J magnitudes are negligible (0.06mag in both cases).

As can be seen from the right panel of figure 2, all the objects with circum-substellar disks have sufficient excess in W1-W2 ( $3.4\ \mu\text{m}$ - $4.6\ \mu\text{m}$ ) to stand clear of the objects with no disks clustered along the isochrone. A few of the objects with disks exhibit a lesser, but still significant colour excess in W1-W2 (i.e. they are more than  $2\sigma$  away from the isochrone). The method successfully discriminated between the 13 class II and 22 class III objects in this sample.

#### 4.1.3 W3 ( $12\ \mu\text{m}$ )

Colours that utilise the longer wavelength W3 ( $12\ \mu\text{m}$ ) passband are of limited use as only 39 of the 116 objects have a  $S/N > 5.0$  in W3. By contrast, all 116 objects have a  $S/N > 8.0$  in W1 and W2. The 39 objects with a  $S/N > 5.0$  in W3 were further examined in the (W1-W2,W3) colour-magnitude diagram shown in figure 3. They are all among the higher mass objects in the sample, as evidenced by the lack of objects around the lower part of the isochrone. The population with the W1-W2 ( $3.4\ \mu\text{m}$ - $4.6\ \mu\text{m}$ ) colour excess is again distinct from the population close to the isochrone as in the previous diagrams. The ninth brightest object in W3 now stands clear from the population near the isochrone. While this object is not obviously part of the population with excess in W1-W2 seen in figure 1 and figure 2, it is more than  $2\sigma$  away from the isochrone. On the combined basis of its excess in W1-W2 and its brightness in W3 it appears to have a disk and so is included in the group of class II objects. This object is one of the 2 objects common to both this study and that of Scholz et al. (2007) who note that it has a binary companion at a separation of 12 au.

#### 4.1.4 W4 ( $22\ \mu\text{m}$ )

The objects also had their detection in the W4 ( $22\ \mu\text{m}$ ) WISE passband examined. Photospheric emission from brown dwarfs is negligible by comparison with emission from a disk at wavelengths longer than  $20\ \mu\text{m}$  (Scholz et al. 2007).

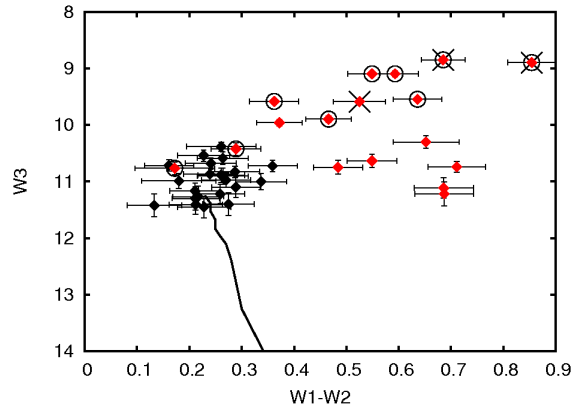


**Figure 3.** (W1-W2,W3) colour-magnitude diagram for 39 of the 116 objects with a  $S/N > 5.0$  in W3 ( $12\ \mu\text{m}$ ). Symbols and isochrone are as in figure 1. The 39 objects are all among the higher mass objects in the sample, as evidenced by the lack of objects around the lower part of the isochrone.

Therefore any object with a bright unambiguous signal in W4 shows clear evidence of the presence of a dusty disk, even if it does not have an excess in W1-W2 ( $3.4\ \mu\text{m}$ - $4.6\ \mu\text{m}$ ). 105 of the objects were not distinguishable from the background in W4, having  $S/N$  varying from 4.7 to zero. The remaining 11 were detected with  $S/N > 5.0$  and have the brightest signals in W4. These 11 are marked with rings in figures 1, 2, 3 and 4. Of the 11, 7 are in the population of 22 with distinct W1-W2 ( $3.4\ \mu\text{m}$ - $4.6\ \mu\text{m}$ ) colour excess.

#### 4.1.5 (W1-W2, J-K)

The (W1-W2,J-K) colour-colour diagram in figure 4 was examined to see if class II and class III objects could be clearly separated. Apart from the 2 objects which are bright in W4 and have large differences in their UKIDSS and 2MASS J magnitudes, none of the objects show any significant excess in J-K. This serves to confirm previous findings (Natta & Testi 2001; Natta et al. 2002) that the efficacy of using J-K excess as a diagnostic for the presence of disks around very low mass stars and brown dwarfs is very limited.

## 4.2 Variable Objects

A comparison was also made of the UKIDSS and 2MASS photometry for each object. UKIDSS and 2MASS data were gathered at different epochs several years apart - 2MASS between 1997 and 2001 (Skrutskie et al. 2006) and UKIDSS from 2005 onwards (Lawrence et al. 2007). Of the 116 objects, 112 showed a variation of less than 0.2 mag in J, H

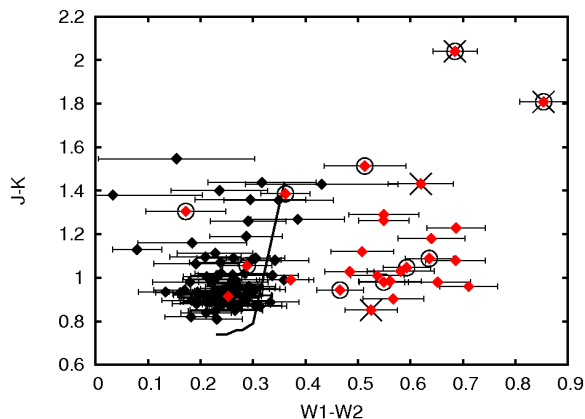


**Figure 4.** (W1-W2,J-K) colour-colour diagram with brown dwarfs and isochrones as in figure 1 and figure 2. The two objects which are bright in W4 and which show signs of accretion have an excess in both W1-W2 and J-K. Apart from those two the rest of the population with excess in W1-W2 shows no obvious excess in J-K.

and K. The remaining 4, which are listed in Table 1 (and marked with crosses in figures 1, 2, 3 and 4), showed variations of greater than 0.2 mag in J, H or K. Such variations in J have been interpreted by Scholz et al. (2009) as signatures of accretion. Scholz et al. (2009) further note that cool spots (comparable to sunspots) are expected to produce variations of  $< 0.15$  mag in J and  $< 0.1$  mag in K while large-scale photometric variability with amplitudes declining towards longer wavelengths - as displayed by the 3 most variable objects in Table 1 - is generally caused by hotspots or variable extinction due to a rotating disk. Hotspots in young stars and brown dwarfs are thought to be a direct consequence of accretion and so they are evidence of the existence of a disk. Likewise, variable extinction is also evidence of the existence of a disk. All 4 objects are in the population with W1-W2 colour excess.

## 5 DISCUSSION

In all, 22 objects were identified as class II objects on the basis of their W1-W2 colour alone. 1 object with a small W1-W2 excess was also placed in the population of class II objects because of its bright W3 signal. A further 4 other objects with no W1-W2 excess were also categorised as class II because of their bright signals in the  $22 \mu\text{m}$  W4 passband. All 27 objects are listed in Table 2. The remaining 89 objects, which are listed in Table 3, were deemed to be class III i.e. they have no disks or disks with a large inner opacity hole of at least 5 - 20AU (see Scholz et al. (2007)). We show the spectral energy distributions for 6 characteristic examples of the class II objects in Appendix B.

### 5.1 Disk Fraction

The overall disk fraction is 27 out of 116 or  $23\% \pm 5\%$  (the uncertainty corresponds to a  $1\sigma$  confidence interval based on binomial statistics). As noted in section 2 above, contamination in our sample appears to be negligible. Conservatively

assuming that 10% of the objects are contaminants which do not exhibit mid-infrared excess would only increase the disk fraction to 27/104, i.e. 26%. This contrasts with the previous results for UpSco of  $37 \pm 9\%$  (Scholz et al. 2007) obtained with a smaller sample of 35 objects. The sample of 35 objects in Scholz et al. (2007) was selected from the surveys of Ardila et al. (2000) (12 objects) and Martin et al. (2004) (23 objects). The higher disk fraction reported in Scholz et al. (2007) may be the result of using a smaller sample of objects or of a possible bias.

The results of Scholz et al. (2007) were also in contrast to the disk fraction of 19% for K0 to M5 stars in the same region obtained by Carpenter et al. (2006) using a sample of 127 K0 to M5 stars. Our new result, of  $23\% \pm 5\%$ , from a similarly sized sample of 116 objects, is statistically indistinguishable from the result of Carpenter et al. (2006), suggesting that disk lifetimes in UpSco for objects later than K0 show no dependency on the mass of the central object. We note that from our sample of 27 disks, 22 (from 72, 31%) are found to be in the mass range  $0.01$ - $0.05 M_{\odot}$ , while only 5 (from 44, 11%) are in the mass range  $0.05$ - $0.09 M_{\odot}$ . This may indicate a trend towards higher disk fractions for very low mass brown dwarfs, but it is not sufficiently robust to warrant further discussion.

#### 5.1.1 Disk Fractions In Other Clusters

This result for UpSco can be compared with those for Cha I (Damjanov et al. 2007; Luhman et al. 2005), IC348 (Luhman et al. 2005; Lada et al. 2006) and  $\sigma$  Ori (Hernandez et al. 2007), 3 other associations for which similar information is available. Damjanov et al. (2007) reports a disk fraction of  $52\% \pm 6\%$  from a sample of 81 K3 to M8 objects in Cha I, while Luhman et al. (2005) finds a disk fraction of  $50\% \pm 17\%$  from a much smaller sample of 18 objects later than M6. Luhman et al. (2005) also finds a disk fraction of  $42\% \pm 13\%$  for 24 objects later than M6 in IC348, where Lada et al. (2006) reports a disk fraction of  $47\% \pm 12\%$  in the range of K6 to M2 stars. In an analysis of disks in  $\sigma$  Ori, Hernandez et al. (2007) finds a disk fraction of  $36\% \pm 4\%$  for stars in the mass range of  $0.1$  to  $1.0 M_{\odot}$  and  $33\% \pm 10\%$  for brown dwarfs (defined as objects  $< 0.1 M_{\odot}$ ). The spectral type of the most massive stars in this range defined by Hernandez et al. (2007) are a little earlier than K (up to G8). However, the vast bulk of their sample is in the mass range of K and M stars, so their result is noted here as being valid for K and M stars in  $\sigma$  Ori. Figure 5 shows that in the wake of this revision of the results for UpSco, all 4 associations now show similar disk fractions for K/M stars and brown dwarfs. Thus, average disk lifetime does not appear to be dependent on the mass of the central object in any of these regions.

#### 5.1.2 The Ages Of The Associations

All the associations listed above are young, i.e.  $< 10$  Myr old. Preibisch et al. (2002) determined an age of about 5 Myr for UpSco, while a revised age of 10 Myr has been proposed by Pecaute et al (2012). Cha I, IC348 and  $\sigma$  Ori have each had various ages of between 2 and 5 Myr reported for each of them

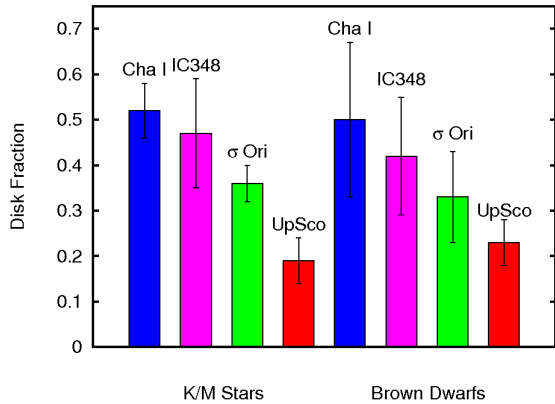


**Figure 5.** Disk fractions for K/M stars compared to disk fractions for brown dwarfs in Cha I, IC348,  $\sigma$  Ori and UpSco. In each case the disk fraction for the K/M stars is statistically indistinguishable from the disk fraction for the brown dwarfs (see text; section 5.1).

(Luhman 2004, 2007; Luhman et al. 2003; Mayne et al. 2007; Zappero Osorio et al. 2002; Oliveira et al. 2002; Sherry et al. 2004). So while UpSco appears to be the oldest of the 4 associations, Cha I, IC348 and  $\sigma$  Ori cannot yet be readily distinguished in terms of their ages. Ergo, apart from stating that the oldest association has the smallest disk fraction, no robust correlation can be safely determined in respect of the disk fractions and ages of the 4 associations.

## 5.2 Transition disks

Objects with very little or no excess at near- to mid-infrared wavelengths but exhibiting excess at longer wavelengths are best understood by assuming an opacity hole in the inner disk (see section 5.3). They may be in the process of clearing dust from their inner disks (Calvet et al. 2002; Muzerolle et al. 2006). Such objects are often termed ‘transition disks’, but the criteria used to define transition disks differ in the literature (see Luhman & Mamajek (2012); Merin et al. (2010) for a discussion of the various criteria). Here we use the term to identify objects with little or no excess in W1-W2, i.e. shortwards of  $10 \mu\text{m}$ , but bright W3 and/or W4 signals (see Sect. 4.1.3 and 4.1.4). The five objects that satisfy this criterion are included in the class II group and may be in the process of a transition from class II to class III.

We do not find any object that might be called a ‘pre-transitional disk’ (Espaillat et al. 2008, 2012), showing evidence for an opacity gap (as opposed to an inner hole) in the disk, i.e. with excess at  $< 10 \mu\text{m}$ , no excess at  $12 \mu\text{m}$ , and excess again at  $22 \mu\text{m}$ .

Based on our adopted definition, the fraction of transition disks around class II brown dwarfs in our sample is 5/27 or 19%. Due to the small sample size, the uncertainty in this number is in the range of  $\pm 10\%$ . Taking this into account, the value is consistent with most previous estimates for the transition disk fraction for low-mass stars which are, for criteria similar to the one adopted here, in the range of 0-20% (e.g., Ercolano, Clarke & Robitaille (2009); Muzerolle et al. (2010)). Thus, based on our estimate for the brown dwarf

regime, there is no evidence for a mass-dependence in the transition disk frequency.

The small number of transition disks in our sample indicates that the transition phase lasts only a short time compared with the total lifetime of the disks. Assuming the upper limit for the age spread of 2 Myr (Preibisch & Zinnecker 1999), we obtain an upper limit of 0.4 Myr for the transition timescale, i.e. about one order of magnitude shorter than the disk lifetime. Thus a two timescale model for the evolution of the disks, as often adopted for low-mass stars, is required for brown dwarfs as well.

## 5.3 Radiative Transfer Models

Scholz et al. (2007) produced model spectral energy distributions based on Monte Carlo radiative transfer simulations for the 13 class II objects that they found in UpSco. Figure 6 shows the spectral energy distributions of the 2 of those objects recovered in this work, which have been recreated using the original model parameters. Data shown for the J, H, K, 9, 10, 11 and  $24 \mu\text{m}$  wavelengths is taken from that of Scholz et al. (2007). The new data for the W1, W2 and W3 passbands is also shown overplotted on the two spectral energy distribution diagrams. It is clear from figure 6 that the data for W1 ( $3.4 \mu\text{m}$ ), W2 ( $4.6 \mu\text{m}$ ) and W3 ( $12 \mu\text{m}$ ) agree very well with both original models, lying on or very close to the modelled flux for a combined photosphere and disk (solid lines in figure 6).

Models of the inner part of a disk rely on observational data in the mid infrared to refine their accuracy. Scholz et al. (2007) noted that the gap in their data coverage in the  $3\text{--}8 \mu\text{m}$  region restricted their ability to constrain the size of any inner disk holes in sources that exhibited excesses at  $9 \mu\text{m}$  and beyond. The addition of the W1 and W2 datapoints for the two objects in figure 6 now allows the accuracy of the models in this region to be probed.

The data for the object in the left panel was originally fitted with a model which included an excess in the mid infrared which necessitated the presence of an optically thick inner disk. The newly overplotted W1 ( $3.4 \mu\text{m}$ ) and W2 ( $4.6 \mu\text{m}$ ) values observed by WISE conform with that part of the model, further indication that a significant W1-W2 excess is evidence for the presence of a disk. The W1-W2 excess for this object places it more than  $4\sigma$  away from the isochrone in the (W1-W2,Z) colour-magnitude diagram in figure 1.

The diagram in the right panel of figure 6 is for the object noted in sections 4.1.3 and 5.2 above that may be in the process of transition from class II to class III. Its lesser excess at W1 and W2 is clear, as is its relatively greater excess at W3. Again, the accuracy of the original model at these wavelengths is confirmed by the newly observed WISE values. While the model shown does preclude the existence of an optically thick inner disk, it does not require the presence of an evacuated hole in the inner disk. Instead, a reduced scale height, i.e. a flatter inner disk is sufficient. This evolution to a flatter disk could be caused by grain growth and dust settling along the lines proposed by Dullemond & Dominik (2004). Ergo, in this model, the process of transition from class II to class III that may be occurring around this object’s disk does not require the pres-



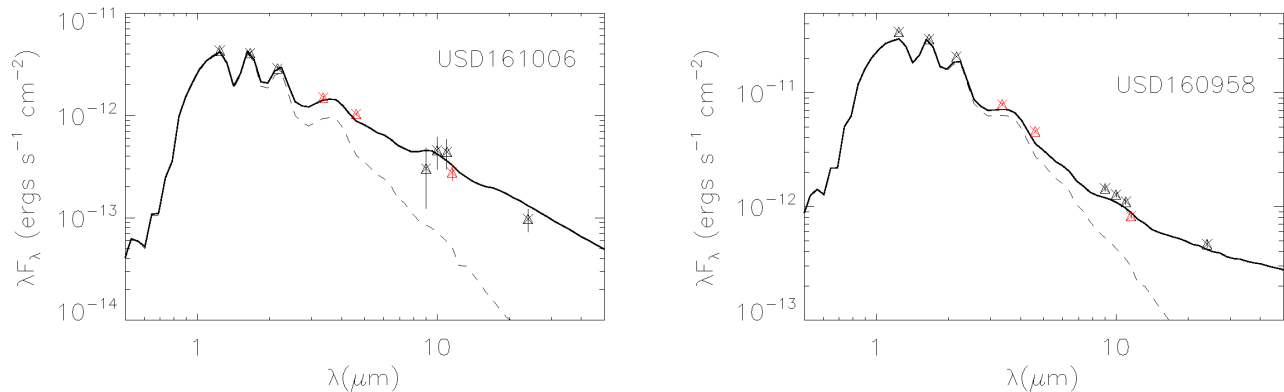


**Figure 6.** Spectral energy distribution for the two class II objects originally identified in Scholz et al. (2007) and recovered in this work. Data shown is taken from that of Scholz et al. (2007) for the J, H, K, 9, 10, 11 and 24  $\mu\text{m}$  wavelengths, along with the newly acquired W1, W2 and W3 values. The Monte Carlo radiative transfer simulations shown for comparison use the same parameters as were given in Scholz et al. (2007). The dotted lines depict calculated photospheric flux while the solid lines represent combined photospheric and disk flux.

ence of mechanisms (e.g. planet formation) that would completely clear the inner disk.

#### 5.4 Comparison with Riaz 2012

In a recent paper Riaz et al. (2012) analyse a sample of 43 spectroscopically confirmed very low mass members (spectral types M4-M8.5) in UpSco using WISE data. They find 6 new class II objects and recover 4 others previously recorded by Scholz et al. (2007) and a further 2 that were found by Slesnick et al. (2008). These 12 objects are listed in their Table 1. We have been kindly provided with a table which includes the 31 other brown dwarfs that they investigated and categorised as class III by B. Riaz (private communication). From the 12 class II and 31 class III objects that they list, there are 12 in common to both that study and ours. Both studies categorise the same 5 objects as class II and the same 7 objects as class III.

Also included in the table supplied by B. Riaz are 6 other objects with  $S/N < 3.0$  in the W3 passband. Riaz et al. (2012) rely on the use of the W3 signal and require that a source have a W3  $S/N \geq 3.0$ . As a result they do not categorise these 6 brown dwarfs. However, using the W1-W2 colour as a primary diagnostic instead of W3 allows a larger range of objects to be successfully examined. All 116 objects investigated in our work have a  $S/N > 8$  in the W1 and W2 passbands, while only 64 of them have a  $S/N \geq 3.0$  in the W3 passband. The 6 objects which cannot be categorised in Riaz et al. (2012) because they have a weak W3 signal have been determined in this work to be class III objects using their W1 and W2 signals alone.

Requiring that a source have a W3  $S/N$  of  $\geq 3.0$  not only restricts the number of objects in any sample from UpSco, it also produces a sample that is biased with respect to the presence of disks. Class III objects in UpSco are less likely than class II objects to have a strong W3 signal. Of the 116 objects examined in this work, 78% of the class II objects, but only 48% of the class III objects have a W3  $S/N$  of  $\geq 3.0$ . Restricting the analysis to those 64 objects only would

have yielded an artificially high disk fraction of 33%, rather than the 23% found from the larger unbiased sample of 116 objects, while also increasing the statistical errors. For these reasons our disk fraction is a more representative value for the brown dwarf population in UpSco.

#### 5.5 Comparison with Luhman & Mamajek 2012

Another recent paper focused on the disks of UpSco members has been published by Luhman & Mamajek (2012). Similar to Riaz et al. (2012) they look at a sample of spectroscopically confirmed members. Their list of targets includes 387 objects with spectral types M4-M8 and another 23 with M8-L2 and is thus substantially larger than the Riaz et al. sample. They analyse the available Spitzer and WISE photometry for these objects. To identify the objects with disks, they use the spectral regime from 4.5 to 24  $\mu\text{m}$ , similar to this paper.

48 of their targets also appear in our total sample of 119, among them 13 classified as class II in this paper. In most cases, our class II/III distinction agrees with the one in Luhman & Mamajek (2012). The only exception is the M9-L1 object 2MASSJ16082847-2315103, which clearly fulfills our class II criterion based on its W1-W2 colour, whereas Luhman & Mamajek (2012) conclude that it is diskless based on its K-W2 colour. At these late spectral types, however, the intrinsic colours of young brown dwarfs increase significantly with spectral type and cover a broad range, i.e. it is challenging to unambiguously distinguish between class II and class III. Whether this source does or does not have infrared excess emission remains to be determined, but this does not affect our results in any way.

The remainder of our sample (71 in total, among them 14 with disks) is new and not covered by Luhman & Mamajek (2012), i.e. our work increases the sample of brown dwarfs analysed with mid-infrared data significantly.

The disk fraction derived by Luhman & Mamajek (2012) for very low mass and substellar members of Up-

Scor is  $\sim 25\%$ , and thus agrees very well with our own result. They also find that disk fractions increase from very small values for B-G stars ( $\leq 10\%$ ) to  $25\%$  for  $\geq M5$  objects. This seems at odds with our own statement of spectral type-independent disk fractions, but a more detailed examination shows that the two studies actually give consistent results for K and M stars.

Luhman & Mamajek (2012) report disk fractions of 6/67 for K0-M0, 35/231 for M0-M4, 97/387 for M4-M8 and 4/23 for M8-L2. To compare with our own values, we calculated the binomial confidence intervals for their disk fractions and obtain  $14 \pm 3\%$  for K0-M4 and  $25 \pm 3\%$  for M4 to L2. This is consistent with the numbers quoted in Sect. 5.1. (19% for K0-M5 and 23% for our sample of brown dwarfs). Note that the uncertainties quoted above only give the statistical confidence interval and do not take into account possible biases (e.g., age spread across the region, uncertainties in spectral types). Thus, based on the current samples, the evidence for a mass dependence of the disk fraction for objects later than K0 is marginal at best.

## 6 CONCLUSIONS

We have carried out a survey for disks around a homogeneous sample of 119 brown dwarfs, the majority of which have not been previously discussed in the literature, in the 5 Myr old UpScor star forming region using photometry from WISE. Contamination in the sample appears to be negligible and the method of selection is unbiased with respect to the presence of disks.

Examining all the UKIDSS, 2MASS and WISE colour-magnitude and colour-colour combinations shows that the WISE W1-W2 colour is the best primary diagnostic for the presence of a disk around the objects.

27 class II objects are identified from the sample. 22 were classified via their W1-W2 colour excess alone. 5 other objects were also categorised as class II from their W3 and/or W4 signals. These 5 objects (19% of all disks) appear to be in the transition phase between class II and class III, leading to the conclusion that this phase is short lived, lasting less than 0.4 Myr, an estimate that is consistent with findings for low-mass stars.

The disk fraction is found to be  $23\% \pm 5\%$ . This fraction is statistically indistinguishable from results for K/M stars in UpScor. Results from the literature for Cha I, IC348 and  $\sigma$  Ori show that their brown dwarf disk fractions are also indistinguishable from their K/M star disk fractions. Therefore the average lifetime of the disks in each of these regions shows no obvious dependency on the mass of the central object. Combined with the short transitional phase from class II to class III, this suggests that the evolution of brown dwarf disks follows “a two timescale model”, similar to low mass stars.

## ACKNOWLEDGEMENTS

The authors would like to thank Isabelle Baraffe of Exeter University and France Allard of the Centre de Recherche Astrophysique de Lyon for supplying model data. This work was supported by Science Foundation Ireland

within the Research Frontiers Programme under grant no. 10/RFP/AST2780. This publication makes use of data products from the Wide-field Infrared Survey Explorer, which is a joint project of the University of California, Los Angeles, and the Jet Propulsion Laboratory/California Institute of Technology, funded by the National Aeronautics and Space Administration. This publication also makes use of data products from the Two Micron All Sky Survey, which is a joint project of the University of Massachusetts and the Infrared Processing and Analysis Center/California Institute of Technology, funded by the National Aeronautics and Space Administration and the National Science Foundation. We would also like to thank the UKIDSS Team for the excellent database they have made available to the community.

## REFERENCES

- Ardila D., Martin E., Basri G., 2000, *AJ*, 120, 479.  
 Carpenter J.M., Mamajek E.E., Hillenbrand L.A., Meyer M.R., 2006, *ApJ*, 651, L49.  
 Calvet N., D’Alessio P., Hartmann L., Wilner D., Walsh A., Sitko M., 2002, *ApJ*, 568, 1008C.  
 Chabrier G., Baraffe I., Allard F., Hauschildt P., 2000, *ApJ*, 542, 464.  
 Cutri R.M., Wright E.L., Conrow T., Bauer J., Benford D., Brandenburg H., Dailey J., Eisenhardt P.R.M., Evans T., Fajardo-Acosta S., Fowler J., Gelino C., Grillmair C., Harbut M., Hoffman D., Jarrett T., Kirkpatrick J.D., Leisawitz D., Liu W., Mainzer A., Marsh K., Masci F., McCallon H., Padgett D., Ressler M.E., Royer D., Shrutskie M.F., Stanford S.A., Wyatt P.L., Tholen D., Tsai C.W., Wachter S., Wheelock S.L., Yan L., Alles R., Beck R., Grav T., Masiero J., McCollum B., McGehee P., Papin M., Wittman M., 2012, Explanatory Supplement to the WISE All Sky Data Release.  
 Damjanov I., Jayawardhana R., Scholz A., Ahmic M., Nguyen D.C., Brandeker A., van Kerkwijk M.H., 2007, *ApJ*, 670, 1337D.  
 Dawson P., Scholz A., Ray T.P., 2011, *MNRAS*, 418, 1231D.  
 de Bruijne J.H.J., Hoogerwerf R., Brown A.G.A., Aguilar L.A., de Zeeuw P.T., 1997, in Perryman M.A.C., Bernacca P.L., Battrick B., eds, in *ESA SP-402: Hipparcos - Venice ’97 Improved Methods for Identifying Moving Groups*. p. 575.  
 Dullemond C.P., Hollenbach D., Kamp I., D’Alessio P., 2007, *Protostars and Planets V*. Univ. Arizona Press, Tucson, p. 555.  
 Dullemond C.P., Dominik C., 2004, *A&A*, 421, 1075D.  
 Ercolano B., Clarke C.J., Robitaille T.P., 2009, *MNRAS*, 394L, 141E.  
 Espaillat C., Calvet N., Luhman K.L., Muzerolle J., D’Alessio P., 2008, *ApJ*, 682L, 125E.  
 Espaillat C., Ingleby L., Hernandez J., Furlan E., D’Alessio P., Calvet N., Andrews S., Muzerolle J., Qi C., Wilner D., 2012, *ApJ*, 747, 103E.  
 Haisch K.E.jr., Lada E.A., Lada C.J., 2001, *ApJ*, 553, L153.  
 Hernandez J., Hartmann L., Megeath T., Gutermuth R., Muzerolle J., Calvet N., Vivas A.K., Briceño C., Allen L., Stauffer J., 2007, *ApJ*, 662, 1067H.



**Table 2.** Positions, UKIDSS Z and J photometry, WISE W1, W2, W3 and W4 photometry of the 27 class II objects. Objects are listed in order of decreasing mass, based on their Z magnitude. Coordinates are J2000.

Name	R.A.	Dec.	Z Mag.	J Mag.	W1 Mag.	W2 Mag.	W3 Mag.	W4 Mag.
2MASSJ16075049-2125200	16:07:50.49	-21:25:20.2	14.03	12.69	11.27	10.73	9.10	7.22
2MASSJ15465432-2556520	15:46:54.32	-25:56:52.1	14.16	12.75	11.40	10.81	9.10	6.23
2MASSJ16052875-2655496	16:05:28.75	-26:55:49.7	14.18	12.89	11.67	11.21	9.90	8.03
2MASSJ16095852-2345186	16:09:58.52	-23:45:18.7	14.20	12.57	11.34	10.97	9.96	8.73*
2MASSJ16030235-2626163	16:03:02.36	-26:26:16.4	14.46	13.12	11.44	10.92	9.59	8.04*
2MASSJ15470374-2601183	15:47:03.74	-26:01:18.4	15.02	13.32	12.03	11.74	10.42	7.39
2MASSJ16134880-2509006	16:13:48.81	-25:09:00.7	15.04	13.56	11.96	11.32	9.55	7.58
2MASSJ15514709-2113234	15:51:47.09	-21:13:23.5	15.12	13.54	10.56	9.88	8.85	7.41
2MASSJ16035573-2738248	16:03:55.73	-27:38:25.1	15.19	13.80	12.70	12.45	12.13*	7.89
2MASSJ15472572-2609185	15:47:25.73	-26:09:18.5	15.40	13.55	11.87	11.51	9.58	7.37
2MASSJ16145253-2718557	16:14:52.53	-27:18:55.7	15.65	14.06	12.34	11.79	10.63	8.70*
2MASSJ15412655-2613253	15:41:26.55	-26:13:25.4	15.65	14.00	12.59	12.10	10.75	8.24*
2MASSJ15521088-2125372	15:52:10.88	-21:25:37.4	15.72	13.86	11.01	10.15	8.90	6.92
2MASSJ16143287-2242133	16:14:32.87	-22:42:13.5	15.82	14.16	12.88	12.34	11.74*	8.38*
2MASSJ15501958-2805237	15:50:19.58	-28:05:23.9	16.04	14.56	13.28	12.72	12.03*	8.98*
2MASSJ16080745-2345055	16:08:07.45	-23:45:05.6	16.06	14.40	12.86	12.21	10.30	8.43*
2MASSJ15524513-2705560	15:52:45.13	-27:05:56.1	16.16	14.42	13.06	12.35	10.74	8.66*
2MASSJ15571880-2711567	15:57:18.81	-27:11:56.8	16.39	14.78	13.42	12.86	11.90*	9.05*
2MASSJ16142144-2339146	16:14:21.44	-23:39:14.8	16.59	14.97	13.57	12.99	11.95*	8.25*
2MASSJ16012238-2708194	16:01:22.39	-27:08:19.5	16.68	14.70	13.24	12.55	11.11	8.43*
2MASSJ16100608-2127440	16:10:06.08	-21:27:44.1	16.82	14.82	13.29	12.65	11.90*	8.72*
2MASSJ15541998-2135428	15:54:19.99	-21:35:43.0	16.85	14.98	13.26	12.57	11.22	8.39*
2MASSJ16083048-2335109	16:08:30.49	-23:35:11.0	16.95	14.88	13.37	12.86	11.69*	8.63*
2MASSJ16082847-2315103	16:08:28.47	-23:15:10.4	17.64	15.45	13.77	13.22	12.21*	8.34*
2MASSJ15472282-2139141	15:47:22.82	-21:39:14.3	17.97	15.65	13.69	13.07	11.63*	8.67*
2MASSJ15433947-2535549	15:43:39.47	-25:35:54.9	18.15	15.77	13.91	13.73	10.77	7.78
2MASSJ15553614-2546591	15:55:36.15	-25:46:59.2	18.23	15.83	13.63	13.12	11.10*	7.92

\*S/N &lt; 5.

- Jayawardhana R., Coffey J., Scholz A., Brandeker A., van Kerkwijk M.H., 2006, *ApJ*, 648, 1206J.
- Lada C.J., Muench A.A., Luhman K.L., Allen L., Hartmann L., Megeath T., Myers P., Fazio G., Wood K., Muzerolle J., Rieke G., Siegler N., Young E., 2006, *AJ*, 131, 1574.
- Lawrence A., Warren S.J., Almaini O., Edge A.C., Hambly N.C., Jameson R.F., Lucas P., Casali M., Adamson A., Dye S., Emerson J.P., Foucaud S., Hewett P., Hirst P., Hodgkin S.T., Irwin M.J., Lodieu N., McMahon R.G., Simpson C., Smail I., Mortlock D., Folger M., 2007, *MNRAS*, 379, 1599.
- Lodieu N., Hambly N.C., Jameson R.F., 2006, *MNRAS*, 373, 95.
- Lodieu N., Hambly N.C., Jameson R.F., Hodgkin S.T., Carraro G., Kendall T.R., 2007, *MNRAS*, 374, 372.
- Lodieu N., Hambly N.C., Jameson R.F., Hodgkin S.T., 2008, *MNRAS*, 383, 1385.
- Lodieu N., Dobbie P.D., Hambly N.C., 2011, *A&A*, 527A, 24L.
- Luhman K.L., Stauffer J.R., Muench A.A., Rieke G.H., Lada E.A., Bouvier J., Lada C.J., 2003, *ApJ*, 593, 1093L.
- Luhman K.L., 2004, *ApJ*, 602, 816L.
- Luhman K.L., Lada C.J., Hartmann L., Muench A.A., Megeath S.T., Allen L.E., Myers P.C., Muzerolle J., Young E., Fazio G.G., 2005, *ApJ*, 631L, 69L.
- Luhman K.L., 2007, *ApJS*, 173, 104L.
- Luhman K.L., Mamajek E.E., 2012, *ApJ*, 758, 31L.
- Martin E.L., Delfosse X., Guieu S., 2004, *AJ*, 127, 449.
- Mayne N.J., Naylor T., Littlefair S.P., Saunders E.S., Jeffries R.D., 2007, *MNRAS*, 375, 1220M.
- Merin, B., Brown J.M., Oliveira I., Herczeg G.J., van Dishoeck E.W., Bottinelli S., Evans N.J.II., Cieza L., Spezzi L., Alcalá J.N., Harvey P.M., Blake G.A., Bayo A., Geers V.G., Lahuis F., Prusti T., Augereau J-C., Olofsson J., Walter F.M., Kuenley C., 2010, *ApJ*, 718, 1200M.
- Muzerolle J., Adame L., D'Alessio P., Calvet N., Luhman K.L., Muench A.A., Lada C.J., Rieke G.H., Siegler N., Trilling D.E., Young E.T., Allen L., Hartmann L., Megeath S.T., 2006, *ApJ*, 643, 1003M.
- Muzerolle J., Allen L., Megeath S.T., Hernandez J., Gutermuth R.A., 2010, *ApJ*, 708, 1107M.
- Natta A., Testi L., 2001, *A&A*, 376L, 22N.
- Natta A., Testi L., Comern F., D'Antona F., Baffa C., Comoretto G., Gennari S., 2002, *A&A*, 393, 597.
- Oliveira J.M., Jeffries R.D., Kenyon M.J., Thompson S.A., Naylor T., 2002, *A&A*, 382L, 22O.
- Pecaut M.J., Mamajek E.E., Bubar E.J., 2012, *ApJ*, 746, 154P.
- Preibisch T., Zinnecker H., 1999, *AJ*, 117, 2381P.
- Preibisch T., Brown A.G.A., Bridges T., Guenther E., Zinnecker H., 2002, *AJ*, 124, 404.
- Riaz B., Lodieu N., Goodwin S., Stamatellos D., Thompson M., 2012, *MNRAS*, 420, 2497R.
- Scholz A., Jayawardhana R., Wood K., Meeus G., Stelzer B., Walker C., O'Sullivan M., 2007, *ApJ*, 660, 1517.
- Scholz A., Xu X., Jayawardhana R., Wood K., Eislöffel J., Quinn C., 2009, *MNRAS*, 398, 873S.

**Table 3.** Positions, UKIDSS Z and J photometry, WISE W1, W2, W3 and W4 photometry of the 89 class III objects. Objects are listed in order of decreasing mass, based on their Z magnitude. Coordinates are J2000.

Name	R.A.	Dec.	Z Mag.	J Mag.	W1 Mag.	W2 Mag.	W3 Mag.	W4 Mag.
2MASSJ16175608-2856399	16:17:56.09	-28:56:40.0	14.01	12.76	11.76	11.53	10.54	8.17*
2MASSJ16034797-2801319	16:03:47.97	-28:01:31.9	14.03	12.81	11.83	11.62	11.17	9.02*
2MASSJ16105728-2359540	16:10:57.28	-23:59:54.1	14.04	12.80	11.68	11.48	11.72*	8.72*
2MASSJ15554229-2546477	15:55:42.29	-25:46:47.8	14.07	12.65	11.52	11.24	10.93*	8.18*
2MASSJ16055898-2556228	16:05:58.99	-25:56:22.9	14.10	12.59	11.50	11.22	10.83	9.08*
2MASSJ16105429-2309108	16:10:54.29	-23:09:11.1	14.13	12.97	11.88	11.68	11.60*	8.27*
2MASSJ15591513-2840411	15:59:15.12	-28:40:41.3	14.14	12.96	12.00	11.77	12.39*	8.75*
2MASSJ16095217-2136277	16:09:52.17	-21:36:27.8	14.15	12.51	11.33	10.97	10.72	9.14*
2MASSJ16063691-2720548	16:06:36.91	-27:20:54.9	14.16	12.88	11.85	11.60	11.91*	8.73*
2MASSJ15411513-2539447	15:41:15.14	-25:39:44.8	14.16	12.76	11.59	11.37	11.30	8.71*
2MASSJ16033799-2611544	16:03:37.99	-26:11:54.4	14.17	12.98	11.96	11.70	11.22	8.63*
2MASSJ16105499-2126139	16:10:54.99	-21:26:14.0	14.22	12.73	11.56	11.30	10.89	8.53*
2MASSJ16154869-2710546	16:15:48.69	-27:10:54.7	14.22	12.82	11.69	11.40	11.65*	8.86*
2MASSJ15450519-2559047	15:45:05.20	-25:59:04.7	14.23	12.90	11.76	11.54	12.00*	8.53*
2MASSJ16072196-2358452	16:07:21.96	-23:58:45.3	14.24	12.99	11.86	11.64	11.27	8.79*
2MASSJ16152819-2315439	16:15:28.19	-23:15:44.1	14.24	13.12	12.08	11.90	11.78*	8.18*
2MASSJ16370523-2625439	16:37:05.24	-26:25:44.0	14.27	12.96	11.96	11.69	11.40	8.91*
2MASSJ15492909-2815384	15:49:29.08	-28:15:38.6	14.29	12.96	11.85	11.63	12.05*	8.91*
2MASSJ15491602-2547146	15:49:16.02	-25:47:14.6	14.31	13.01	11.87	11.60	10.90	8.20*
2MASSJ16082229-2217029	16:08:22.29	-22:17:03.0	14.31	12.94	11.85	11.56	11.10	8.81*
2MASSJ16061595-2218279	16:06:15.95	-22:18:28.0	14.31	13.17	12.11	11.91	11.92*	9.02*
2MASSJ15544260-2626270	15:54:42.61	-26:26:27.0	14.32	13.05	11.91	11.72	11.61*	8.23*
2MASSJ16090168-2740521	16:09:01.68	-27:40:52.3	14.33	12.86	11.71	11.44	10.97	8.72*
2MASSJ15582376-2721435	15:58:23.76	-27:21:43.7	14.35	13.07	12.02	11.79	11.37*	8.78*
2MASSJ16132180-2731219	16:13:21.80	-27:31:22.0	14.36	13.25	11.93	11.85	11.60*	8.77*
2MASSJ15415562-2538465	15:41:55.63	-25:38:46.5	14.37	13.10	12.02	11.79	12.14*	8.93*
2MASSJ16002535-2644060	16:00:25.35	-26:44:06.1	14.38	13.02	11.90	11.66	11.67*	8.50*
2MASSJ15545410-2114526	15:54:54.11	-21:14:52.7	14.40	13.26	12.10	11.94	10.71	8.31*
2MASSJ16062637-2306113	16:06:26.37	-23:06:11.4	14.48	13.20	12.12	11.87	11.68*	8.90*
2MASSJ16121609-2344248	16:12:16.09	-23:44:25.0	14.50	13.19	11.96	11.78	10.99	8.21*
2MASSJ16090451-2224523	16:09:04.51	-22:24:52.5	14.57	12.92	11.66	11.40	10.59	8.23*
2MASSJ16113470-2219442	16:11:34.70	-22:19:44.3	14.61	13.24	12.11	11.87	12.25*	8.77*
2MASSJ15505993-2537116	15:50:59.94	-25:37:11.7	14.62	13.33	12.30	12.05	11.55*	8.90*
2MASSJ15524857-2621453	15:52:48.57	-26:21:45.4	14.62	13.30	12.27	12.00	12.51*	9.14*
2MASSJ16372782-2641406	16:37:27.83	-26:41:40.7	14.63	13.30	12.14	12.00	11.42	8.95*
2MASSJ15522943-2721003	15:52:29.44	-27:21:00.4	14.64	13.47	12.45	12.14	12.36*	9.06*
2MASSJ15530374-2600306	15:53:03.75	-26:00:30.7	14.66	13.43	12.36	12.14	12.03*	8.62*
2MASSJ15493660-2815141	15:49:36.59	-28:15:14.3	14.66	13.39	12.36	12.05	11.63*	8.79*
2MASSJ16133476-2328156	16:13:34.76	-23:28:15.7	14.74	13.48	12.39	12.12	11.77*	8.81*
2MASSJ15490803-2839550	15:49:08.02	-28:39:55.2	14.82	13.60	12.45	12.21	10.68	8.15*
2MASSJ16112630-2340059	16:11:26.30	-23:40:06.1	14.83	13.40	12.16	11.92	12.04*	8.55*
2MASSJ15495733-2201256	15:49:57.33	-22:01:25.7	14.89	13.35	12.15	11.89	11.56*	8.64*
2MASSJ16062870-2856580	16:06:28.70	-28:56:58.2	14.90	13.52	12.39	12.18	11.41	9.06*
2MASSJ15572692-2715094	15:57:26.93	-27:15:09.5	14.93	13.66	12.59	12.39	12.00*	9.10*
2MASSJ16164539-2333413	16:16:45.39	-23:33:41.6	14.99	13.73	12.62	12.33	11.61*	8.44*
2MASSJ16005265-2812087	16:00:52.66	-28:12:09.0	15.04	13.57	12.48	12.27	11.79*	9.13*
2MASSJ16132665-2230348	16:13:26.66	-22:30:35.0	15.05	13.52	12.33	11.99	11.00	8.82*
2MASSJ16115737-2215066	16:11:57.37	-22:15:06.8	15.07	13.67	12.51	12.24	11.76*	8.84*
2MASSJ16064910-2216382	16:06:49.10	-22:16:38.4	15.09	13.73	12.63	12.37	11.90*	8.79*
2MASSJ15585793-2758083	15:58:57.93	-27:58:08.5	15.13	13.81	12.78	12.54	12.08*	9.06*
2MASSJ15420830-2621138	15:42:08.31	-26:21:13.8	15.15	13.74	12.59	12.32	12.10*	9.07*
2MASSJ16090197-2151225	16:09:01.98	-21:51:22.7	15.16	13.59	12.32	12.08	10.87	8.45*
2MASSJ16124692-2338408	16:12:46.92	-23:38:40.9	15.18	13.60	12.42	12.19	12.20*	8.25*
2MASSJ16153648-2315175	16:15:36.48	-23:15:17.6	15.19	13.93	12.85	12.61	12.03*	8.23*
2MASSJ16134264-2301279	16:13:42.64	-23:01:28.0	15.19	13.72	12.47	12.25	12.20*	8.38*
2MASSJ16113837-2307072	16:11:38.37	-23:07:07.5	15.19	13.74	12.60	12.31	11.97*	8.59*
2MASSJ15583403-2803243	15:58:34.03	-28:03:24.5	15.21	13.72	12.53	12.30	11.45	9.03*
2MASSJ16192399-2818374	16:19:23.99	-28:18:37.5	15.29	13.79	12.73	12.40	11.51*	8.57*
2MASSJ15490414-2120150	15:49:04.14	-21:20:15.2	15.31	13.77	12.64	12.37	11.50*	8.92*
2MASSJ16051243-2624513	16:05:12.43	-26:24:51.4	15.40	14.06	12.93	12.76	12.29*	9.08*
2MASSJ15533067-2617307	15:53:30.68	-26:17:30.7	15.49	13.99	12.83	12.60	12.06*	8.64*

**Table 4.** Table 3 continued.

Name	R.A.	Dec.	Z Mag.	J Mag.	W1 Mag.	W2 Mag.	W3 Mag.	W4 Mag.
2MASSJ15544486-2843078	15:54:44.85	-28:43:07.9	15.51	14.12	12.99	12.81	12.60*	8.90*
2MASSJ15531698-2756369	15:53:16.98	-27:56:37.2	15.53	13.96	12.84	12.55	12.50*	8.58*
2MASSJ15551960-2751207	15:55:19.59	-27:51:21.0	15.60	14.03	12.93	12.67	12.30*	9.10*
2MASSJ15564227-2646467	15:56:42.28	-26:46:46.8	15.62	14.03	12.85	12.54	11.65*	8.51*
2MASSJ16101316-2856308	16:10:13.15	-28:56:31.0	15.67	14.06	12.89	12.59	12.16*	9.09*
2MASSJ16115439-2236491	16:11:54.39	-22:36:49.3	15.73	14.27	13.04	12.80	11.86*	8.32*
2MASSJ16092938-2343121	16:09:29.39	-23:43:12.2	15.96	14.20	12.94	12.65	12.30*	8.98*
2MASSJ16103014-2315167	16:10:30.14	-23:15:16.8	16.06	14.37	13.05	12.75	11.97*	8.35*
2MASSJ15561721-2638171	15:56:17.21	-26:38:17.2	16.10	14.52	13.26	13.00	10.38	8.23*
2MASSJ16072641-2144169	16:07:26.41	-21:44:17.1	16.17	14.60	13.43	13.17	12.26*	8.55*
2MASSJ16142061-2745497	16:14:20.61	-27:45:49.8	16.31	14.49	13.22	12.93	12.26*	8.69*
2MASSJ15572820-2708430	15:57:28.21	-27:08:43.0	16.40	14.78	13.71	13.47	12.21*	8.77*
2MASSJ16134079-2219459	16:13:40.79	-22:19:46.1	16.49	14.72	13.42	13.08	12.05*	8.99*
2MASSJ15442275-2136092	15:44:22.75	-21:36:09.3	16.55	15.01	13.69	13.48	11.68*	8.55*
2MASSJ15543065-2536054	15:54:30.65	-25:36:05.5	16.73	15.03	13.80	13.61	11.58*	8.17*
2MASSJ16064818-2230400	16:06:48.18	-22:30:40.1	16.82	14.93	13.63	13.37	12.04*	8.68*
2MASSJ15444172-2619052	15:44:41.72	-26:19:05.3	17.16	15.21	13.86	13.63	12.26*	8.86*
2MASSJ16072382-2211018	16:07:23.82	-22:11:02.0	17.24	15.20	13.70	13.41	12.20*	8.87*
2MASSJ16104714-2239492	16:10:47.13	-22:39:49.4	17.44	15.26	13.80	13.51	12.02*	8.57*
2MASSJ16084744-2235477	16:08:47.44	-22:35:47.9	17.74	15.69	14.30	14.11	12.28*	8.79*
2MASSJ15491331-2614075	15:49:13.32	-26:14:07.5	18.29	16.04	14.50	14.12	12.16*	8.88*
2MASSJ16081843-2232248	16:08:18.43	-22:32:25.0	18.51	16.10	14.28	14.05	11.56*	8.72*
2MASSJ16195827-2832276	16:19:58.26	-28:32:27.8	18.74	16.18	14.42	14.10	12.47*	8.77*
2MASSJ15451990-2616529	15:45:19.91	-26:16:53.0	18.77	16.27	14.41	14.06	11.85*	8.20*
2MASSJ16362646-2720024	16:36:26.47	-27:20:02.5	18.77	16.33	14.52	14.22	11.44*	8.79*
2MASSJ16360175-2703305	16:36:01.75	-27:03:30.5	19.12	16.64	14.95	14.91	12.07*	8.86*
2MASSJ16073799-2242468	16:07:37.99	-22:42:47.0	19.24	16.76	15.16	14.73	12.51*	8.25*
2MASSJ15504498-2554213	15:50:44.99	-25:54:21.4	19.90	16.93	14.86	14.70	11.84*	8.33*

\*S/N &lt; 5.

- Sherry W.H., Walter F.M., Wolk S.J., 2004, AJ, 128, 2316S.
- Skrutskie M.F., Cutri R.M., Stiening R., Weinberg M.D., Schneider S., Carpenter J.M., Beichman C., Capps R., Chester T., Elias J., Huchra J., Liebert J., Lonsdale C., Monet D.G., Price S., Seitzer P., Jarrett T., Kirkpatrick J.D., Gizis J., Howard E., Evans T., Fowler J., Fullmer L., Hurt R., Light R., Kopan E.L., Marsh K.A., McCallon H.L., Tam R., Van Dyck S., Wheelock S., 2006, AJ, 131, 1163.
- Slesnick C.L., Carpenter J.M., Hillenbrand L.A., 2006, AJ, 131, 3016.
- Slesnick C.L., Hillenbrand L.A., Carpenter J.M., 2008, ApJ, 688, 377S.
- Wright E.L., Eisenhardt P.R.M., Mainzer A.K., Ressler M.E., Cutri R.M., Jarrett T., Kirkpatrick J.D., Padgett D., McMillan R.S., Skrutskie M., Stanford S.A., Cohen M., Walker R.G., Mather J.C., Leisawitz D., Gautier T.N.III., McLean I., Benford D., Lonsdale C.J., Blain A., Mendez B., Irace W.R., Duval V., Liu F., Royer D., Heinrichsen I., Howard J., Shannon M., Kendall M., Walsh A.L., Larsen M., Cardon J.G., Schick S., Schwalm M., Abid M., Fabinsky B., Naes L., Tsai C.-W., 2010, AJ, 140, 1868W.
- Zapatero Osorio M. R., Bejar V.J.S., Pavlenko Ya., Rebolo R., Allende Prieto C., Martn E.L., Garca Lpez R.J., 2002, A&A, 384, 937Z.

## APPENDIX A: NEW OBJECTS FROM UKIDSS 9TH DATA RELEASE

This appendix outlines the method used to identify new brown dwarfs in UpSco using the UKIDSS 9th Data Release. It is the same method used by Dawson, Scholz & Ray (2011) to analyse the 8th Data Release. For the sake of brevity, some of the details described by Dawson, Scholz & Ray (2011) are not repeated here.

UKIDSS is made up of several components including the Galactic Cluster Survey (GCS). Described in detail in Lawrence et al. (2007) the GCS is a survey of ten large open star clusters and star forming regions, including UpSco.

The instrument used to take the GCS images is the Wide Field Camera (WFCAM). Data collected by the WFCAM is subject to an automated process that detects and parameterises objects and performs photometric and astrometric calibrations. The resulting reduced image frames and catalogues are then placed in the WFCAM Science Archive (WSA). The WSA can be interrogated using Structured Query Language (SQL).

As shown in figure A1, the new area in UpSco investigated here and surveyed for the 9th Data Release covers 24deg<sup>2</sup>. The data for objects in the target area were obtained via an SQL query to the UKIDSS GCS database. All queries were structured to include only point source objects in order to avoid contamination by extended sources (e.g. relatively nearby galaxies). As every object with photometric characteristics consistent with a brown dwarf had its proper motion assessed, in order to check whether it is likely

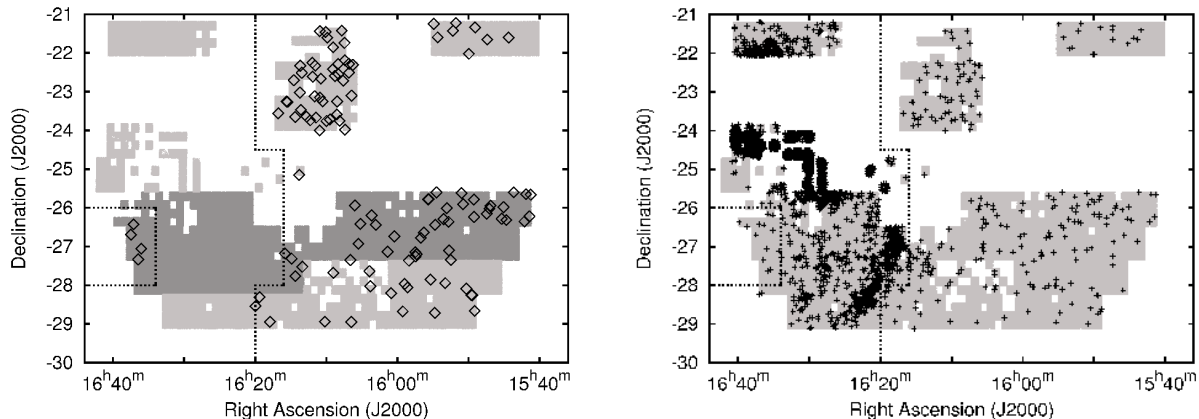


**Figure A1.** Coverage in Z, Y, J, H and K filters of  $57 \text{ deg}^2$  in Upper Scorpius from the UKIDSS GCS. The left panel shows the new  $24 \text{ deg}^2$  of coverage from the 9th Data Release in dark grey and earlier coverage in light grey. The open diamonds mark the position of the 116 brown dwarfs that comprise the sample analysed in this work. The right panel shows the location of objects selected by the first cut in the  $(Z-J,Z)$  colour-magnitude diagram. 95% of all the objects selected from the 9th Data Release are clustered around the heavily extinguished region surrounding  $\rho$  Oph. To obtain a minimally contaminated sample of brown dwarf candidates, the area inside the two sets of dashed lines was excluded from consideration.

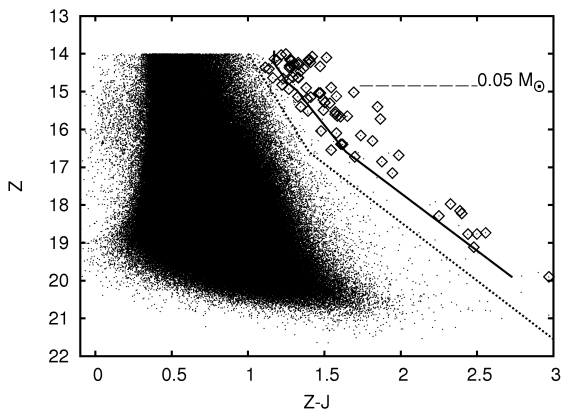


**Figure A2.**  $(Z-J,Z)$  colour-magnitude diagram showing the 76 brown dwarf candidates from the 9th Data Release as open diamonds. All other objects are shown as small dots. The 5 Myr DUSTY model (Chabrier et al. 2000) isochrone is also shown with mass decreasing going down the isochrone from  $0.09 M_{\odot}$  at the top to  $0.01 M_{\odot}$  at the bottom. The  $0.05 M_{\odot}$  position on the isochrone is indicated. All objects to the left of the dashed line were rejected because of their colours.

a member of UpSco, each query submitted also correlated all objects found in the UKIRT GCS databases with those found in 2MASS databases. The 2MASS data is used as a first epoch for the purposes of proper motion calculation.

### A1 Photometry

A query similar to that shown in Dawson, Scholz & Ray (2011) was submitted to the WSA. The query returned 1,438,887 objects.

The objects were assessed on the basis of their position on a  $(Z-J,Z)$  colour-magnitude diagram as shown in figure A2. To refine the search, a new query was submitted to the WSA eliminating all objects to the left of a line in the  $(Z-J,Z)$  colour-magnitude diagram from  $(Z-J,Z) = (1.0,$

$14.0)$  through  $(1.4, 16.6)$  to  $(3.0, 21.55)$  (dashed line in figure A2). This query left 4,398 objects. Reddening caused by extinction shifts objects to the right and down on colour-magnitude diagrams. To assess if reddening was contaminating the results the 4,398 objects had their location plotted as shown in the right panel of figure A1. There is an obvious clustering of objects in a large area which coincides with the heavily extinguished region around  $\rho$  Oph. Therefore, the analysis was confined to 706,638 objects in the 9th Data Release that were outside that region (dashed lines in figure A1). This left only 200 of the 4,398 objects selected in the initial  $(Z-J,Z)$  cut. These 200 objects were examined again in the  $(Z-J,Z)$  colour-magnitude diagram. 86 of the objects to the left of the line  $(Z-J,Z) = (1.1, 14.0)$  through  $(1.1, 14.3)$ ,  $(1.2, 14.9)$ ,  $(1.3, 15.2)$ ,  $(1.6, 17.0)$  to  $(3.0, 21.0)$  were rejected for being too far from the isochrone on the blue side, leaving 114 photometric candidates.

### A2 Proper Motion

The 114 photometric candidates were then examined to find their proper motion. The resulting vector point diagram of UpSco is shown in figure A3. The known proper motions of UpSco in right ascension and declination are about  $-11 \text{ mas/yr}$  and  $-25 \text{ mas/yr}$  respectively (de Bruijne et al. 1997; Preibisch et al. 2002). Of the 114 candidates, 4 were too faint to be recorded in 2MASS leaving 110 candidates with proper motion data calculated. The remaining 110 candidates included 14 with proper motions greater than the range of figure A3.

All 96 candidates shown in figure A3 are predominantly centred around the  $(-11, -25)$  position. A  $2\sigma$  selection circle as calculated in Dawson, Scholz & Ray (2011) is shown centred on that position. There is no significant clustering of objects around the  $(0,0)$  position indicating that the sample is not contaminated by more distant objects e.g. AGB stars which have similar surface temperatures and colours to brown dwarfs, but much greater intrinsic luminosities. The 76 candidates within the  $2\sigma$  selection circle were then classi-

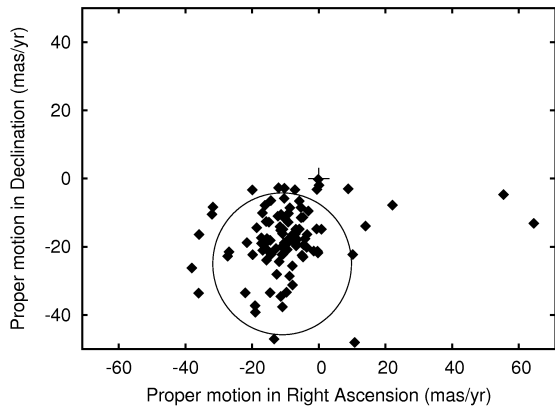


**Figure A3.** Vector point diagram for 96 candidate brown dwarfs in Upper Scorpius. There is an obvious and identifiable cluster around  $(-11, -25)$ , while there is no significant clustering around the origin, indicating that there is very little contamination from background objects in the sample. Candidates lying outside the  $2\sigma$  selection circle were classified as non-members, leaving 76 brown dwarf members of UpSco.

fied as members of UpSco. These objects so selected have the photometric and proper motion characteristics of a 5 Myr old brown dwarf member of UpSco. 25 of the 76 were among the sample of 68 selected by Dawson, Scholz & Ray (2011), yielding 51 new objects from the 9th Data Release to add to the sample. From these 51 brown dwarfs, 5 have been identified before. Lodieu et al. (2006) identifies 1 of them, Martin et al. (2004) lists another and Ardila et al. (2000) identifies 3. We note that the remaining 46 have not been previously identified in other surveys.

One potential caveat with respect to this sample is the fact that the Upper Scorpius population and the younger  $\rho$ Oph population are unlikely to be clearly separated in colour-magnitude or proper motion diagrams. By avoiding the areas with very high extinction (see figure A1) we exclude the bulk of the population of  $\rho$ Oph, but some scattered young substellar members of  $\rho$ Oph might still contaminate our sample. The low disk fraction in our sample, however, suggests that this cannot be a major factor.

## APPENDIX B: SELECTED SPECTRAL ENERGY DISTRIBUTIONS

In this appendix we show spectral energy distributions for 12 objects from our sample, 6 class II and 6 class III objects for comparison. The class III objects used have the closest magnitude in the J passband to the class II objects with which they are compared. Shown in the top panels of figure B1 are 2 of the typical examples that were deemed class II on the basis of their W1-W2 ( $3.4\mu\text{m}$ - $4.6\mu\text{m}$ ) colour alone (as is the object featured in the left panel in figure 6). The difference in slopes between the W1 and W2 points on the class II and class III spectral energy distributions are apparent, as are the higher W3 ( $12\mu\text{m}$ ) and W4 ( $22\mu\text{m}$ ) values of the class II objects. The 2 class II objects that stand out in figure 4 because of their large J-K excess are shown in the middle panels of figure B1. Of all the 27 class II objects, the spectral energy distributions for these 2 show the

greatest divergence from those of their corresponding class III objects. The bottom panels in figure B1 show 2 of the 5 class II objects that could not be distinguished on the basis of their W1-W2 colour alone. (The right panel in figure 6 features another of these objects). The bottom right panel is the most extreme example of all the 5 objects with little or no W1-W2 excess and deemed class II based on their bright W3 and/or W4 signals (the transition disks). It exhibits no W1-W2 excess and has a weak W3 signal. Apart from its strong W4 signal it resembles a class III object.

This paper has been typeset from a  $\text{T}_{\text{E}}\text{X}/\text{L}^{\text{A}}\text{T}_{\text{E}}\text{X}$  file prepared by the author.

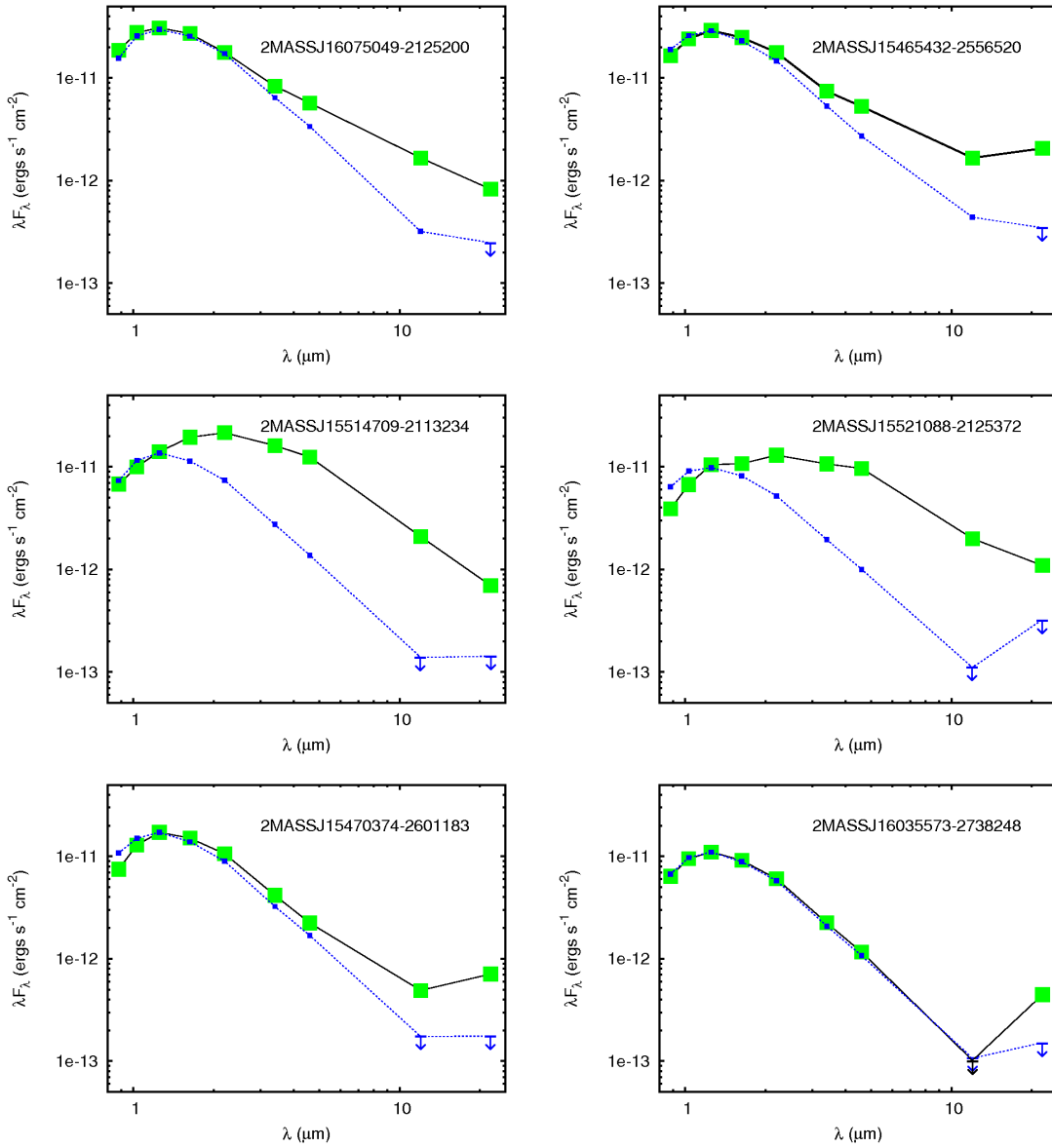


**Figure B1.** Spectral energy distributions for 6 of the 27 class II objects (solid lines with large squares) shown alongside 6 of the 89 class III objects (dotted lines with small squares). Detections with a S/N of < 5.0 are marked as upper limits. The class II objects in the top and middle panels are among the 22 distinguished using their W1-W2 ( $3.4\ \mu\text{m}$ - $4.6\ \mu\text{m}$ ) colour alone. The middle panels show the 2 objects that also have the large J-K excess, as well as having the brightest W3 signals, bright W4 signals and significant photometric variability (see Table 1 ). The class II objects in the bottom panels are 2 of the 5 with little or no W1-W2 excess that are included in the class II group on the basis of their bright W3 and/or W4 signals.